PLEA 2017 EDINBURGH

Design to Thrive

Cool roof and natural ventilation for UHI mitigation and indoor comfort – cooling indicators for a commercial building

Madi Kaboré[1,2,3], Emmanuel Bozonnet[1,3], Patrick Salagnac[1], Marc Abadie[1] and Rémi Perrin[2]

[1] LaSIE (UMR CNRS 7356), University of La Rochelle, Av. M. Crépeau, 17042 La Rochelle, France ;

[2] SOPREMA, 14 Rue de St Nazaire, 67025 Strasbourg Cedex, France ;

[3] IRSTV (FR CNRS 2488), Nantes, France.

Abstract: This paper proposes a first approach to decision support in the design of passive cooling solutions for buildings in dense urban contexts. The problem of summer discomfort in these buildings must then take into account the effects associated with urban heat islands. The absence of objective criteria constitutes a barrier on the development of solutions such as the radiative treatment of roofs and natural ventilation envisaged here. A simple representation methodology, based on the Sankey diagram and indicators, is proposed and applicated on a typical commercial building. Nocturnal Natural ventilation contributes to a great reduction in summer thermal discomfort compared to the "cool roof". Reflective coatings reduce the anthropogenic heat transferred to the external environment. The cooling potential of the building and the urban environment, thus obtained for different temperate climates shows the prospects for the design of efficient solutions with controlled environmental impacts.

Keywords: Thermal comfort, Natural ventilation, Cool roof, Building Envelope, Urban Heat Island.

Nomenclature

DH	degree-hour, °Ch
h	heat transfer coefficient, $Wm^{-2}K^{-1}$
Q	energy, kWh/m^2
S	area, m^2
t	time, s
T	temperature, °C
U	U value of floor., $Wm^{-2}K^{-1}$
Greek symbol	
η_{FRin}	thermal discomfort indicator
η_{FRout}	indicator of the external environment
Subscripts	
A	related to air
C	related to heat transferred by convection
I	related to infiltration
g	related to ground
LW	related to LongWave heat transfer
sky	related to LW heat transfer with sky
SW	related to ShortWave heat transfer
T	related to heat transmitted by conduction
V	related to ventilation
W_i	related to wall indoor surface
W_o	related to wall outdoor surface
(+)	related to positive value
(-)	related to negative value
Exponents	
heat	related to heating system
i	related to indoor
o	related to outdoor
other	related to internal loads
refl	related to reflected solar radiation
win	related to opennings

Introduction

According to the IPCC, global warming could increase from 1.1 to 6.4 °C by the end of the 21st century according to scenarios (Guivarch and Cassen, 2015). The consequences will be particularly significant in urban areas where the building and its immediate surroundings are the source of multiple microclimate disruptions. The perceptible manifestation of these disruptions is the well-known phenomenon of Urban Heat Island (UHI), which is characterized by an increase in the temperatures of urban sites higher than those of the surrounding countryside. The urban heat island is the mutual response of several factors related to the climate and the specificities of the sites, the design and construction materials of the urban spaces and the way of life of the population (transport). These critical situations are observed during the summer period, with consequences on thermal comfort (indoor and outdoor environments), energy consumption, pollution and more dramatic heat-related health problems particularly in middle latitude countries. The reduction of this vulnerability requires the establishment, as far as possible, of an urbanism and a built environment adapted to high temperature. Mitigation and adaptation solutions are relatively well known (Akbari et al. 2016). They are based on the use of passive cooling technologies at the scale of the building and the restoration of natural cooling at scale of district and city. So building design processes which are focused on indoor environment quality, have to deal also with the issues of UHI and climate change by taking into account the outdoor environment quality. Building Performance Simulation (BPS) tools have become essential in building design processes. However, one of the main barriers to the use of BPS tools is the use of the output data and their complex representation. Decision-makers need simple tools and indicators to which they can refer to evaluate and choose the most effective solutions. These tools and indicators are indispensable for the construction stakeholders and policy key actors. The Sankey diagrams, which are typically used to represent flows of materials or energies, have been developed and used for more than 100 years (Schmidt, 2008) and allow to have an easier representation of the phenomena. However, there are very few cases for building design (Singer and Simon, 2013; O'Brien, 2012; Schmidt, 2008). We are developing this approach in this paper for a typical commercial building with large ground footprint. Commercial buildings account for 7 % of the total world energy consumption (Pérez-Lombard et al., 2008), mostly for heating and cooling systems with more than 60 % of the consumption (Carvalho et al., 2010). Here investigations are conducted on the interaction between the envelope and its surrounding environment as well as the quality of the indoor environment during hot periods by proposing an urban cooling indicator. This indicator makes it possible to evaluate the performance of cooling solutions with regard to the indoor and outdoor environments and compare them. Passive cooling solutions such as cool roofing and natural ventilation are then qualified and compared for different climates.

Methodology

Description of the case study

The building (Figure 1), 6 m high, consists of a steel structure with a floor area of 36 × 36 m^2. This building is located in an urban area subject to temperate climates (Strasbourg, Paris and Marseille). The vertical walls are composed of 1.3 cm of plaster, 14 cm of mineral wool, and a 2 mm steel sheet. The windows consist of 30 m² glass surfaces located on the east, west and south facades. The 13.5 cm thick roof (1.3 cm of plaster, 12 cm of glass wool, 2 mm of steel cladding) has skylights (8 % of the surface area of the roof). The floor is made up to 16 cm of concrete (0.5 m^{2}K/W) and the soil is sandy. The inertia of the shelves and partitions is considered as an internal mass. For this reference building, the roof has a solar reflectance of 0.3 and the thermal emissivity is 0.9. The building air permeability level is equivalent to

2 cm^2/m^2 which is representative of a common steelconstruction building (Persily, 1998). An occupation density of 11.6 m^2/person is considered here (Deru et al., 2011). The occupancy period is 07:00 AM - 10:00 PM every day except on Sundays (empty building). Artificial lighting is turned off if natural daylighting exceeds 300 lux. A heating system is set to maintain the indoor temperature to a minimum of 19 °C when the building is occupied and 5 C otherwise. No cooling system is present in this prototypical building. A heat recovery ventilation (HRV) system provides 0.5 air changes per hour (ACH) when the occupants are present.

Building thermal model

The thermal simulations of the building were carried out by coupling thermal model (TRNSYS©) to airflow model (CONTAM©). The rates of infiltration and natural ventilation are induced by wind and thermal effects. The wind pressure coefficient on the envelope is determined by the model proposed by (Swami and Chandra, 1988). The heat transfer with the ground is modeled according to a three-dimensional approach (Lapisa, Bozonnet, Abadie and Salagnac, 2013). An additional complete year is used to initialize each calculation.

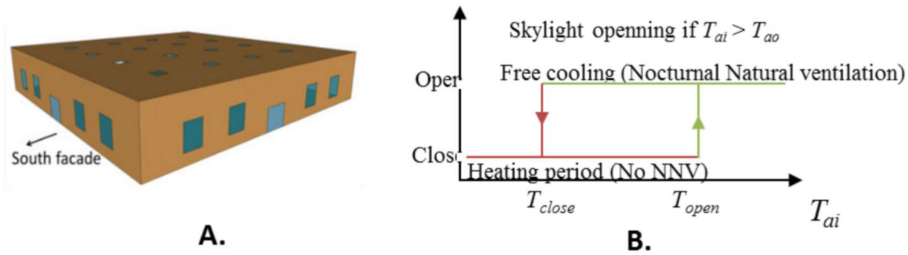

Figure 1: Mock-up of the studied building (A); Control of heating system and night ventilation (B)

Modeling of cooling techniques

Passive cooling techniques have been used to cool the building in summer: cool roof (CR), nocturnal natural ventilation (NNV) and the combination of both (CR + NNV). A "cool roof" is a roof covering layer that limits the absorption of solar irradiance by a high solar reflectivity; while emitting the accumulated heat towards the sky due to its high thermal emissivity. Here, a solar reflectivity of 0.7 was considered while maintaining the emissivity of the reference case (0.9). Nocturnal natural ventilation (NNV) is ensured by opening ad-hoc vents in the lower part of the building and the skylights located on the roof during the warm periods from 11 pm to 6 am (periods of unoccupancy and without additional mechanical ventilation) and when the indoor temperature is above outside temperature (deviation of 2 °C). The mechanical ventilation operates during the summer and can be adjusted according to ventilation needs. The control of the opening for the natural ventilation must be done outside the heating periods and thus determined by the control diagram (Figure 1.B). During periods of non-heating (mainly summer), skylights are operated according to outdoor and indoor air temperatures (T_{ao} and T_{ai}). The choice of the limits for heating and natural ventilation periods T_{close} and T_{open} are decisive for both the annual potential of passive cooling and heating needs.

Results

Sankey diagram of the reference case

In this first part, energy flows (Figure 2.A) between the building and its environment are represented by a Sankey diagram (Figure 2.B). This synthetic representation makes it possible to quickly identify the strengths and weaknesses of the components of the energy systems and their integration. Two thermal balances were carried out. The first balance concerns the building envelope (windows, walls and roof), the floot and the internal walls.

$$\underbrace{Q_{SW}}_{1} + \underbrace{\sigma\epsilon S\left(T_{sky}^4 - T_{Wo}^4\right)\Delta t}_{2} + \underbrace{h_C^o S(T_{ao} - T_{\mathrm{Wo}})\Delta t}_{3} + \underbrace{US\,(T_{\mathrm{Wi}} - T_{\mathrm{g}})\Delta t}_{4} + \underbrace{Q_{\mathrm{SW}}^{win} + Q_{LW}^{others}}_{5} + \underbrace{Q_{LW+}^{i} - Q_{LW-}^{i}}_{6} + \underbrace{h_C^i S\left(T_{\mathrm{Sky}} - T_{\mathrm{Wo}}\right)\Delta t}_{7} + \underbrace{\Delta Q_W}_{8} = 0 \quad (1)$$

Where (1) represents the solar radiation towards the building envelope ($Q_{\mathrm{SW}} - Q_{\mathrm{SW}}^{\mathrm{refl}}$); (2) corresponds to longwave (LW) heat transfer between the building skin and the sky (Q_{sky}); (3) is the convective heat transfer between the skin and outdoor air ($Q_{C+}^o - Q_{C-}^o$);

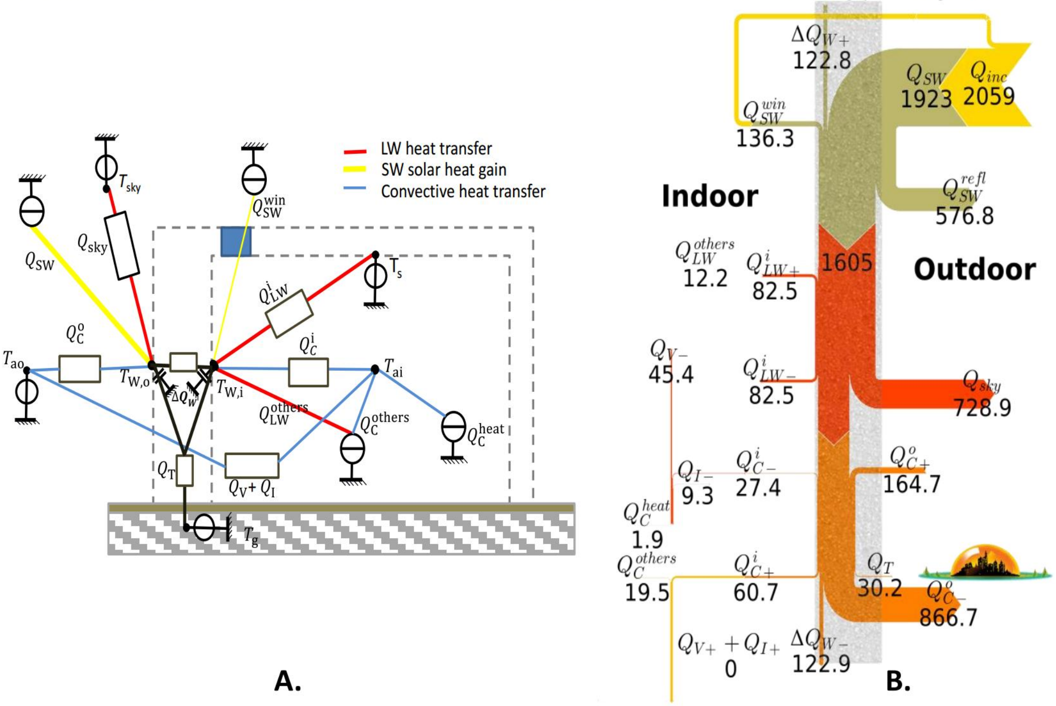

Figure 2: **A.** Heat transfer in the building and between the building and its environment; **B.** Sankey diagram (kWh/m²) of the entire year

(4) is the heat transfer by conduction with the ground (Q_{T}); (5) are the short-wave radiation heat gain through windows and skylights ($Q_{\mathrm{SW}}^{\mathrm{win}}$) and the radiative part the building internal loads ($Q_{\mathrm{LW}}^{\mathrm{others}}$) ; (6) is longwave heat transfer of indoor surfaces ($Q_{LW+}^i - Q_{LW-}^i$); (7) is the convective heat transfer between indoor surfaces and the zone air ($Q_{C+}^i - Q_{C-}^i$) and (8) is a variation of stored energy by the skin, the floor and internal partitions ΔQ_{W}. Equation (1) can take the following form (by separating the positive (+) and the negative (-) inputs) and showing the various terms necessary for the Sankey diagram:

$$Q_{\mathrm{SW}} - Q_{\mathrm{SW}}^{refl} - Q_{\mathrm{LW}}^o + Q_{\mathrm{C+}}^o + Q_{\mathrm{T}} - Q_{\mathrm{C-}}^o + \Delta Q_{\mathrm{W+}} = Q_{\mathrm{SW}}^{win} + Q_{\mathrm{LW}}^{others} + Q_{\mathrm{LW+}}^i - Q_{\mathrm{L-}}^i + Q_{\mathrm{C+}}^i - Q_{\mathrm{C-}}^i + \Delta Q_{\mathrm{W-}} \quad (2)$$

The second balance concerns the air node:

$$\underbrace{(\dot{m}_V + \dot{m}_I)C_p(T_{\mathrm{ai}} - T_{\mathrm{ao}})\Delta t}_{1} + \underbrace{h_C^i S(T_{\mathrm{ai}} - T_{\mathrm{Wi}})\,\Delta t}_{2} + \underbrace{Q_{\mathrm{C}}^{heat} + Q_{\mathrm{C}}^{others}}_{3} = 0 \quad (3)$$

Where (1) shows the heat gain by ventilation and infiltration ($Q_{\mathrm{V+}} + Q_{\mathrm{I+}} - Q_{\mathrm{I-}} - Q_{\mathrm{V-}}$); (2) is the convective heat transfer with indoor surface of walls, floor, roof, windows and partitions ($Q_{\mathrm{C+}}^{\mathrm{i}} - Q_{\mathrm{C-}}^{\mathrm{i}}$); (3) is the convective heat gain due to the heating system ($Q_{\mathrm{C}}^{\mathrm{heat}}$), to occupants and lighting ($Q_{\mathrm{C}}^{\mathrm{others}}$). So this balance becomes:

$$Q_{V+} + Q_{I+} + Q_{C+}^{i} + Q_{C}^{heat} + Q_{C}^{others} - Q_{I-} - Q_{V-} - Q_{C-}^{i} = 0 \quad (4)$$

Figure 2.B shows the Sankey diagram from the annual simulation of the built environment in interaction with the external environment (Marseille climate). All the energies are related to floor area. This diagram makes it possible to analyze the specificities of the dynamic transfers of this building typology (Bozonnet et al., 2016; Lapisa, Bozonnet, Abadie and Salagnac, 2013; Lapisa, Bozonnet, Abadie, Salagnac, et al., 2013). On the other hand, the inertia of the envelope, shelves and the ground which contributes to regulate the temperature in the building is highlighted ($\Delta Q_{W-} = \Delta Q_{W+} = 122.8$ kWh/m^2). We can observed that the convective heat transferred to the nearby environment air ($Q_{C+}^{o} + Q_{C-}^{o}$) and is worth 702 kWh/m^2 a year. This heat transferred to the external environment is detrimental in summer and contributes to the appearance of UHI phenomena. In the following, we will therefore restrict the study of the cooling potential from the Sankey diagram to the cooling needs period of the building.

Cooling indicator for UHI and indoor comfort – definitions and results

In order to characterize the performance of the building with respect to the occupied zone and the surrounding environment, two quantities are used:

- Summer thermal comfort can be evaluated by calculating the degree-hours of discomfort (*DH*) using the maximum adaptive comfort temperature (EN-ISO-15251) as reference.
- During the period when the building needs to be cooled, thermal exchanges between the building and the external surrounding modify the urban microclimate and are represented by the amount of energy (Q^o) exchanged with the outside air.

$$Q^{o} = Q_{C+}^{o} - Q_{C-}^{o} - Q_{I-} - Q_{V-} \quad (5)$$

In the case of Marseille, the cooling needs period corresponds to 6159 hours (70% of a year) for this building. The energy (Q^{o}) transferred to the surrounding environment represents 670 kWh/m² (Figure 3.A) during the cooling period, compared with 757 kWh/m² for the whole year. The number of degree-hours is 10114.2 °Ch. In this case, the ground (27 kWh/m^2) contributes strongly in dissipating heat in the zone. In order to compare the performances of the various cooling techniques, a cooling indicator of the external environment η_{FRout} and thermal discomfort indicator η_{FRin} are calculated by equations (6).

$$\eta_{FRout} = 100\,\frac{Q^{ref} - Q^{o}}{Q^{o,ref}};\ \eta_{FRin} = 100\,\frac{DH_{ref} - DH}{DH_{ref}};\ \Delta C_{EP} = 100\,\frac{C_{EP,ref} - C_{EP}}{C_{EP,ref}} \quad (6)$$

The passive cooling scenarios are compared to the reference case without cooling solution. η_{FRout} is the rate of change of the heat transmitted outwards (Q^{o}). This is the anthropogenic contribution of the building to the local microclimate. η_{FRin} is the rate of change of discomfort's degree-hours. It characterizes the cooling needs of the building. The rate of change in primary energy consumption (ΔC_{EP}) is also calculated in order to evaluate the impact of cooling technology on the energy requirements of the building throughout the year.

Figure 3.B shows a graphical representation of the thermal exchanges for the "Cool Roof" case during the summer period in Marseille. The passive cooling scenarios are compared to the reference case without cooling solution. The presence of this reflective coating decreases the heat absorbed by the roof. This results in a decrease of the surface and air temperatures of the surrounding. The overheating period is reduced for this case and this is reflected in the different integrated flows over this period. A reduction of the discomfort

period is thus obtained with an internal cooling potential η_{FRin} of 4.3 %. The heat transmitted to the nearby environment also decreases to 314.6 vs. 670 kWh/m² for the reference case, i.e. η_{FRout} = 53.1 %.

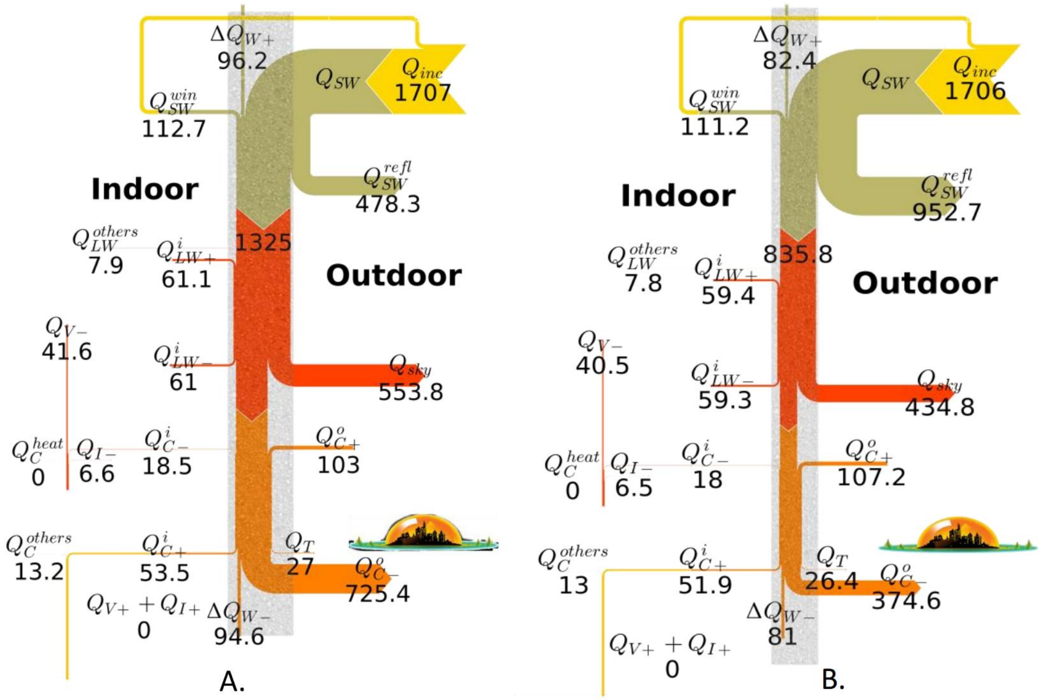

Figure 3 **A.** Sankey diagram (kWh/m²) during the summer period in Marseille; **B.** Sankey diagram (in kWh / m²) - Case of Cool Roof (CR)

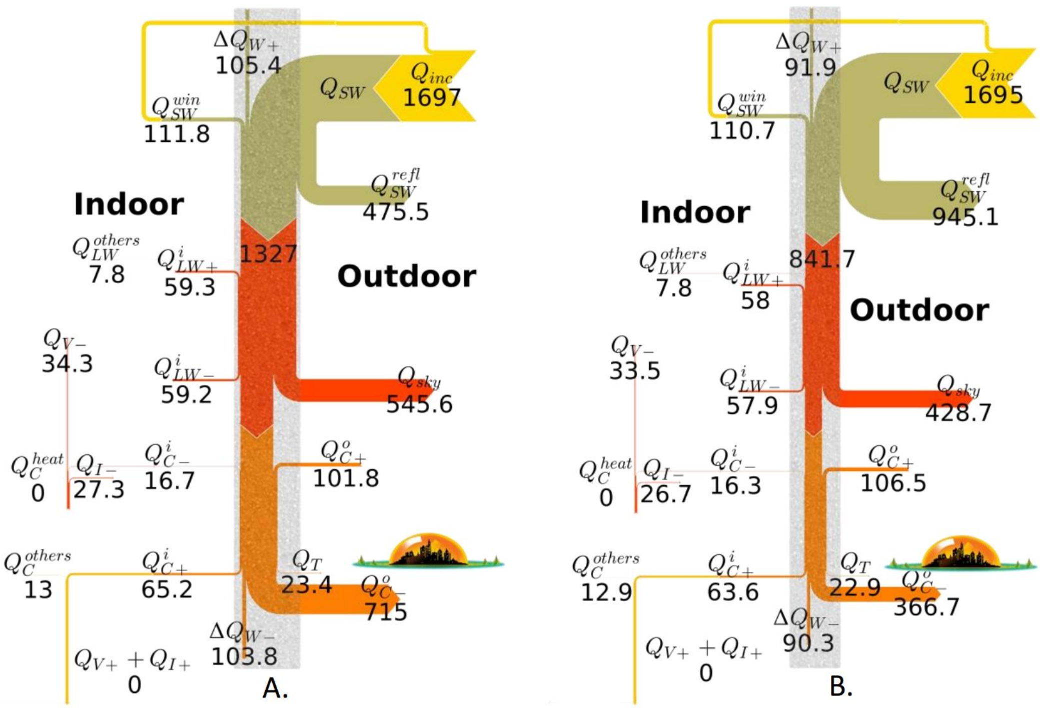

Figure 4: **A.** Sankey diagram (in kWh/m²) - Case of the NNV; **B.** Sankey diagram (in kWh/m²) - Case of CR+ NNV

Figure 4.A shows for the detailed sankey obtained in the case of nocturnal natural ventilation as passive a cooling technique. The nocturnal ventilation (Q_{I-}) makes it possible to

cool down the building surfaces $\left(Q^{i}_{C+}\right)$ thus putting the inertia of the envelope and internal mass (ΔQ_{w+}= 103.8 vs 94.6 kWh/m² for the reference case) to contribution during daytime. It can be observed that the energy dissipated through the ground is lower compared to the reference case. The degree-hours of discomfort falls to 5709,5 °Ch, which represents a cooling potential η_{FRin} of 43.6 % for Marseille. Heat transfer to the outdoor environment increases slightly with η_{FRout} equal to -0.6 %. The results obtained when combining the two previous solutions (NNV + CR) are shown in Figure 4.B. This combination offers best performances both for the indoor and the surrounding external by addind the effects of each passive solution taken standalone. The cooling potentials are η_{FRin} = 46.3 % and η_{FRout} = 52.22 % respectively for the indoor and outdoor.

Climate Impact

In this section, we present the results obtained under other climates (Paris, Strasbourg). Table 1 shows the indicators η_{FRin}, η_{FRout} and ΔC_{EP}. Concerning outdoor cooling, the trends are the same for all the studied climates. The impact of natural ventilation on the energy exchanged with the environment is negligible compared to the cool roof solution. Whatever the temperate climates studied, increasing the albedo of the roof by 0.4, a reduction in the overheating of the environment is achieved, close to 50 %. The performance of the cool roof is low because the roof is isolated. η_{FRin} is low in Marseille because the discomfort degree-hours is higher than the other climates. For the building cooling indicator, natural ventilation allows a higher reduction of the discomfort compared to the "cool roof". However, the use of "cool roof" leads to a slight increase in C_{EP}, mainly due to lower solar heat gain.

Table 1: η_{FRin}, ΔC_{EP}, *and* η_{FRout} for different climates

	Marseille			Paris			Strasbourg		
	η_{FRin}	ΔC_{EP} (%)	η_{FRout}	η_{FRin}	ΔC_{EP} (%)	η_{FRout}	η_{FRin}	ΔC_{EP} (%)	η_{FRout}
CR	4.3	-0.6	53.1	9.7	-0.4	51.2	8.0	-3.7	49.5
NNV	43.6	-1.3	-0.6	81.9	0.4	8.0	68.4	-4.3	2.7
NNV+CR	46.3	-2.3	52.2	85.1	-0.2	53.2	72.2	-4.9	50.6

Conclusion

In this study based on thermal simulations of the building, the passive cooling potential was evaluated both from the point of view of the building indoor environment and also its anthropogenic heat transferred to the environment. The integrated analysis over a full year was presented using the Sankey diagram to visualize the energy flows especially during the cooling needs period. We focused on thermal exchanges in the summer period between the building and its external surrounding and also summer comfort through the implementation of indicators. Through the study of a commercial building, located in temperate climates using this methodology, we have shown the interest of the "cool roof" and natural night ventilation as passive cooling strategies for indoor and outdoor environments. The increase of the cool roof is complementary to the nocturnal ventilation through the skylights. Nocturnal natural ventilation contributes to a great reduction in summer thermal discomfort compared to the "cool roof" (81.9 % instead of 9.7 % for Paris) due to the fact that buildings are insulated in these heating needs climates. Reflective coatings reduce the overheating of the external environment (50 %). For a better efficiency, the combination of these techniques is advantageous. On the other hand, inertia in general and that of the ground in particular constitutes a significant passive cooling sink in temperate climates for this type of building.

Acknowledgements

The authors thank the Region of GRAND EST for its support.

References

Akbari, H., C. Cartalis, D. Kolokotsa, A. Muscio, A.L. Pisello, F. Rossi, M. Santamouris, A. Synnefa, N.H. Wong, et M. Zinzi. 2016. « Local Climate Change and Urban Heat Island Mitigation Techniques - The State of the Art ». *Journal of Civil Engineering and Management* 22 (1): 1‑16. doi:10.3846/13923730.2015.1111934.

Bozonnet, Emmanuel, Remon Lapisa, Patrick Salagnac, et Marc Abadie. 2016. « Low-rise commercial buildings optimization – energy performance and passive cooling potential in France ». In *Building Simulation & Optimization 2016*, 108‑14. Newcastle, England.

Carvalho, M. M. Q., E. L. La Rovere, et A. C. M. Gonçalves. 2010. « Analysis of variables that influence electric energy consumption in commercial buildings in Brazil ». *Renewable and Sustainable Energy Reviews* 14 (9): 3199‑3205. doi:10.1016/j.rser.2010.07.009.

Deru, Michael, Kristin Field, Daniel Studer, Kyle Benne, Brent Griffith, Paul Torcellini, Bing Liu, et al. 2011. « U.S. Department of Energy commercial reference building models of the national building stock ». *Publications (E)*, février, 1‑118.

Guivarch, Céline, et Christophe Cassen. 2015. « L'atténuation du changement climatique : retour sur le 5e rapport du Giec ». *La Météorologie* 8 (88): 97. doi:10.4267/2042/56365.

Lapisa, R., Bozonnet, E., Abadie, M. and Salagnac, P. (2013) 'Effect of ground thermal inertia on the energy balance of commercial low-rise buildings', Building simulation for a sustainable world, Chambéry, France, pp. 2068–3825

Lapisa, R., Bozonnet, E., Abadie, M., Salagnac, P. and Perrin, R. (2013) 'Design impacts of cool roof coating, ventilation and thermal inertia on commercial low-rise building energy demand and summer comfort', Energy conservation technologies for mitigation and adaptation in the built environment: the role of ventilation strategies and smart materials, Athens, Greece, pp. 1061–1070

O'Brien, W. (Liam) (2012) 'Preliminary Investigation of the Use of Sankey Diagrams to Enhance Building Performance Simulation-supported Design', Proceedings of the 2012 Symposium on Simulation for Architecture and Urban Design, SimAUD '12, San Diego, CA, USA, Society for Computer Simulation International, p. 15:1–15:8

Pérez-Lombard, Luis, José Ortiz, et Christine Pout. 2008. « A review on buildings energy consumption information ». *Energy and Buildings* 40 (3): 394‑98. doi:10.1016/j.enbuild.2007.03.007.

Persily, A. K. (1998) Airtightness of commercial and institutional buildings: blowing holes in the myth of tight buildings, Building and Fire Research Laboratory, National Institute of Standards and Technology

Schmidt, Mario. 2008. « The Sankey Diagram in Energy and Material Flow Management ». *Journal of Industrial Ecology* 12 (1): 82‑94. doi:10.1111/j.1530-9290.2008.00004.x.

Singer, S. and Simon, A. J. (2013) EEBHub Building 101 Sankey Diagram Energy Analysis, Report

Swami, M . V, et S. Chandra. 1988. « Correlations for pressure distribution on buildings and calculation of natural - ventilation airflow ». *ASHRAE Transactions* 94: 243‑46.